04

Operating regimes and structure of an atmospheric-pressure interelectrode microwave discharge in argon

© S.N. Antipov, M.Kh. Gadzhiev, M.V. Il'ichev, A.S. Tyuftyaev, V.M. Chepelev, D.I. Yusupov

Joint Institute for High Temperatures, Russian Academy of Sciences,
125412 Moscow, Russia
e-mail: antipov@ihed.ras.ru

Received October 10, 2023
Revised July 1, 2024
Accepted July 2, 2024

Continuous and pulse-periodic operating regimes and spatio-temporal structure of an atmospheric-pressure interelectrode microwave discharge in transverse argon flow were experimentally investigated for a hemisphere-to-plate electrodes configuration. A multielectrode plasma torch with a power of ~ 100 W was used as a gas-discharge device, electromagnetic energy to which was supplied from a waveguide-type microwave plasmatron operating on the basis of a magnetron with a frequency of 2.45 GHz. The discharge regime switching were carried out using a high-voltage three-phase magnetron power supply. In the continuous regime, fractal filamentation of near-electrode regions of a glow-type microwave discharge was described. Diagnostics of the regimes was conducted by floating potential oscillography of the microwave discharge flowing afterglow (cold plasma jet).

Keywords: microwave plasmatron, atmospheric-pressure glow discharge, plasma diagnostics, discharge filamentation.

DOI: 10.61011/TP.2024.10.59357.260-23

Introduction

As is known, non-equilibrium plasma is plasma in a state that differs from the one of complete thermodynamic equilibrium [1]. The key feature of non-equilibrium plasma is that electric energy induces the emergence of energetic electrons without any significant heating of the gas medium. A wide spectrum of radicals and excited particles with high reactivity is produced in this case. This feature is used widely in plasma modification of surface properties of various materials, which include such temperature-sensitive objects as polymers, biological materials, etc. [2]. Low- and reduced-pressure glow discharges (e.g., capacitive RF discharges and DC discharges) have long been used for plasma treatment [3–7]. Plasma in such discharges is characterized by a low density of atoms in the gas phase and, consequently, a low rate of collisions between electrons and heavy particles. Cold plasma jets based on atmospheric-pressure microwave discharges, where excited particles and radicals with high reactivity are produced, have attracted increasing interest in recent years. Notably, the jets themselves do not exert a destructive influence on the material subjected to plasma treatment [8–14]. The so-called „plasma plume," which is a discharge in gas flow in the vicinity of a pointed electrode inside a dielectric tube of a small (~ 1 mm) diameter, is being used and studied most extensively at present [15–23]. This type of single-electrode microwave discharge is close in shape to a torch discharge, which is typical of an RF corona discharge at frequencies of 10 MHz and near-atmospheric pressures.

The treated surface area is an important parameter of the plasma source in various technological processes, such as plasma cleaning, plasma surface activation, plasma deposition, and plasma etching. Such techniques as surface „scanning" or the use of a matrix of discharge tubes are applied in large-area treatment [16,24–27]. At the same time, only a few studies into the discharges suitable for generating wide plasma jets have been published to date. The series of experiments on generation of cold microwave plasma with the MicroPlaster device, which features a plasma torch with six electrodes in a common discharge chamber, is the one most worthy of note here (see, e.g., [27–32]). However, these studies were aimed at determining the characteristics of the flowing afterglow of an argon microwave discharge (cold plasma jet) and the sterilization effect it produces in biomedical applications, and the properties of the discharge itself were left unexamined. The design and characterization of a microwave plasma source of the discussed kind have also been the subject of recent studies [33–36] in which the authors of the present paper were also involved. As for the development of electrodeless sources of wide microwave plasma jets, the experiments [37] with a freely localized non-equilibrium atmospheric-pressure discharge sustained by continuous microwave radiation from a technological gyrotron with a frequency of 24 GHz and a power of $20-5000$ W are worth mentioning. A plasma jet was formed in this case in a gas flow at the quasi-optical microwave beam waist and consisted, in pure argon, of short-lived filamentary plasma formations. When small amounts of CO_2 were introduced into the argon flow, plasma filaments became „blurred", and the discharge assumed a diffuse form.

The results of an experimental study of continuous and pulse-periodic current regimes and the spatiotemporal

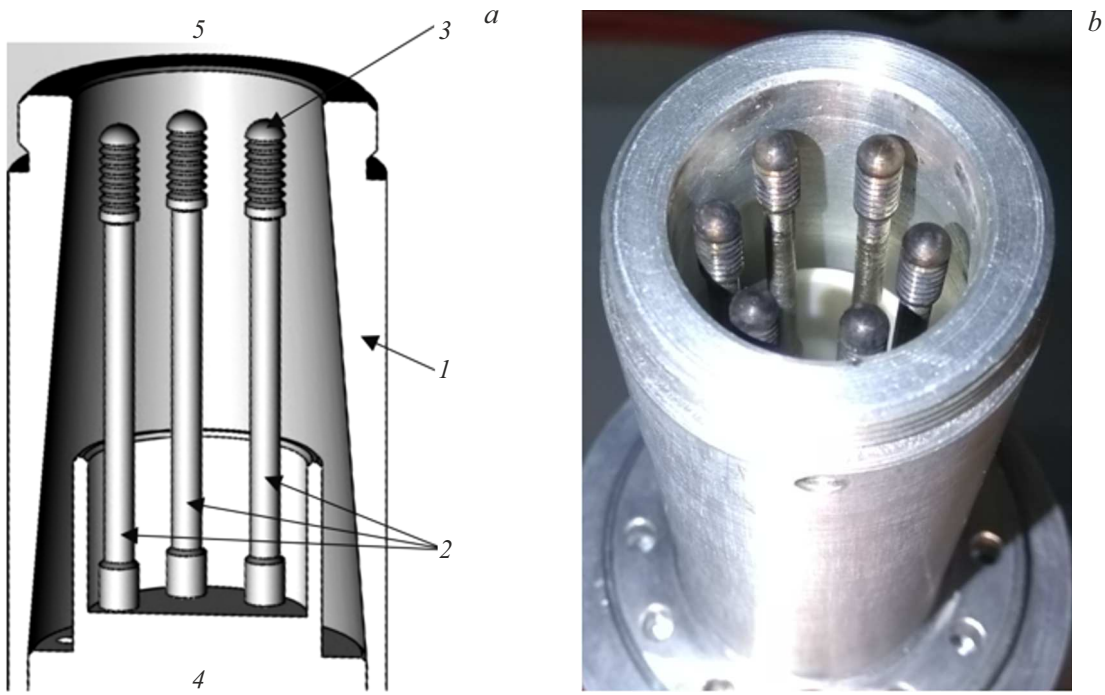

Figure 1. Plasma torch for excitation of an atmospheric-pressure interelectrode microwave discharge in transverse gas flow (*a* — diagram, *b* — photographic image): *1* — cylindrical discharge chamber, *2* — rod electrodes, *3* — region of localization of discharge electrode spots (rounded electrode end), *4* — insulator, and *5* — outlet of the discharge chamber. The diameter of the discharge chamber outlet is 25 mm, the diameter of the rounded electrode end is 4 mm, and the distance between the end of the electrode and the inner wall of the chamber outlet is 2 mm.

structure of an electrode microwave discharge excited in the „hemisphere–plate" interelectrode gap geometry in transverse argon flow at atmospheric pressure are reported below. As was already noted, this discharge has been first obtained with medical and biological applications in mind and constitutes a novel discharge type: atmospheric-pressure glow microwave discharge. A multielectrode plasma torch with a wide outlet, which has been designed earlier, was used as a gas-discharge device. The electric power was supplied to it from a waveguide-type microwave plasmatron [33–36,38].

1. Microwave plasmatron with a plasma torch

The microwave plasmatron used in the present experiments is constructed on the basis of a typical low-power microwave generator (magnetron) with a frequency of 2.45 GHz and a power of 1.1 kW. It allows one to produce atmospheric-pressure microwave discharges both in its own waveguide path (electrodeless configuration) and in an external portable discharge chamber (plasma torch) designed to generate cold plasma jets based on an interelectrode microwave discharge with a power up to several hundred watts [33–36,38]. The microwave plasmatron is a modular system with three key components: a high-voltage three-phase power supply unit (PSU), a microwave unit with a magnetron, and a detachable three-section waveguide path with a water load. The waveguide is made of rectangular steel profile $100 \times 50 \times 2$ mm in size with WR-340 flanges. Tap water is supplied to the cooling and water load circuit.

An induction-type coupler (a coupling loop positioned on the narrow wall of the central waveguide section) is used to power external gas-discharge devices. The design of the coupler allows one to alter the coupling strength by rotating the plane of the loop that is terminated with an N-type coaxial connector. With losses taken into account, the coupler may divert up to 15% of the magnetron power [36]. The plasma torch is the effective load and is connected to the coupler via a cable assembly (50 Ω coaxial cable 2 m in length with two N-type connectors). The torch is designed as a cylindrical discharge chamber with an internal diameter of 25 mm that contains six rod electrodes with a diameter of 4 mm and a length of ≈ 9.2 mm positioned parallel to each other to form an equilateral hexagon in the cross section of the torch (Fig. 1). High-purity argon (99.998%) was used as a plasma-forming gas. Its flow rate was adjusted within the 3–10 *l*/min range. Gas was supplied to the torch from cylinders with flow-metering reducers.

Continuous and pulse-periodic discharge excitation (current) regimes were examined. The three-phase PSU of the plasmatron (380/220 V, 50 Hz) was used to switch between these regimes. The schematic diagram of operation of the radio engineering systems in the PSU is presented in Fig. 2.

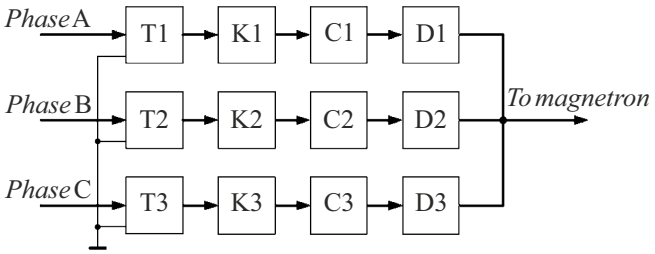

Figure 2. Block diagram of the three-phase magnetron power supply circuit: T1–T3 — step-up transformers, K1–K3 — switches, C1–C3 — capacitor banks, and D1–D3 — diode rectifiers.

The PSU features step-up transformers T1–T3, switches K1–K3, capacitor banks C1–C3, and diode rectifiers D1–D3. The three-phase magnetron power supply circuit was used: the voltage of each phase was fed to a separate step-up transformer, and the alternating secondary-winding voltage of each transformer was close to 2.2 kV. Switches K1–K3 provide an opportunity to adjust the capacity of capacitor banks C1–C3. The greater the capacity of a capacitor bank is, the higher is the electric power of the magnetron and the higher is the power of output microwave radiation. The supply voltage of the magnetron is formed by diode rectifiers D1–D3. Control signals for switches K1–K3 are sent from the PSU control system. All three phases („A," „B", and „C") may be used to power the magnetron. The supply voltage is virtually constant in this case, and the magnetron operates in the continuous regime. When only one or two phases are used, the voltage is supplied with a frequency of 50 Hz. The magnetron then operates in the pulse-periodic regime. The disadvantage of this magnetron operation regime is the lack of an option to adjust the pulse repetition rate, since it is determined by the frequency of the power network.

2. Experimental results and discussion

A microwave discharge in the plasma torch was initiated by seed ionization (short-term introduction of a tip of thin wire with a diameter of 200 μm into the interelectrode gap). The region near the wire tip is characterized by significantly higher field strengths (compared to the values averaged over the entire gap), which leads to gas ionization, the emergence of seed electrons at the tip, and subsequent development of a discharge within the entire interelectrode gap. A spark from external sources, such as a piezoelectric element, Tesla coil, etc., may also be used to initiate a discharge.

The current discharge regimes were examined by measuring the floating potential of a single electric probe in the flowing afterglow of the microwave discharge (cold plasma jet) with an oscilloscope at the torch outlet. The needle contact of the oscilloscope probe was positioned for this purpose near the outlet of the torch on its central axis. The amplitude-time (frequency) characteristics of the floating

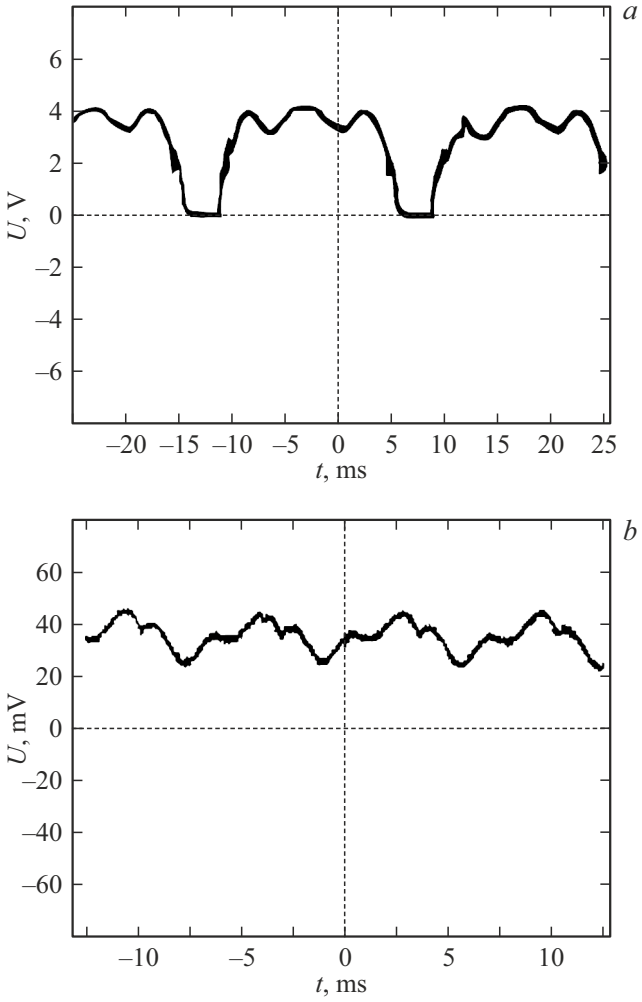

Figure 3. Oscilloscope records of the floating potential in the flowing afterglow of a microwave discharge (cold plasma jet) in pulse-periodic (a) and continuous (b) current regimes.

potential in a plasma jet in continuous and pulse-periodic microwave discharge regimes were obtained this way. The shapes of electric potential at the probe are shown in Fig. 3. It can be seen that the pulse-periodic regime with two-phase power supply is characterized by a frequency of 50 Hz, a pulse duration of approximately 15 ms, and a duty cycle of 4/3. The pulses have a near-rectangular shape with three „humps" with a height of approximately 20% of the maximum value (Fig. 3, a). In the continuous regime, the signal oscillated with a frequency of 150 Hz, which is the effect of three magnetron supply voltage phases (Fig. 3, b). The signal level at a distance of several centimeters from the torch outlet was $\sim 10-100$ mV and could reach several volts in the immediate vicinity of the outlet.

Microwave discharges in the examined regimes were recorded from the side of the torch outlet with a CCD video camera at a rate of 30 frames per second. The following phenomenological description of a microwave discharge in the torch may be provided. In the continuous regime, a

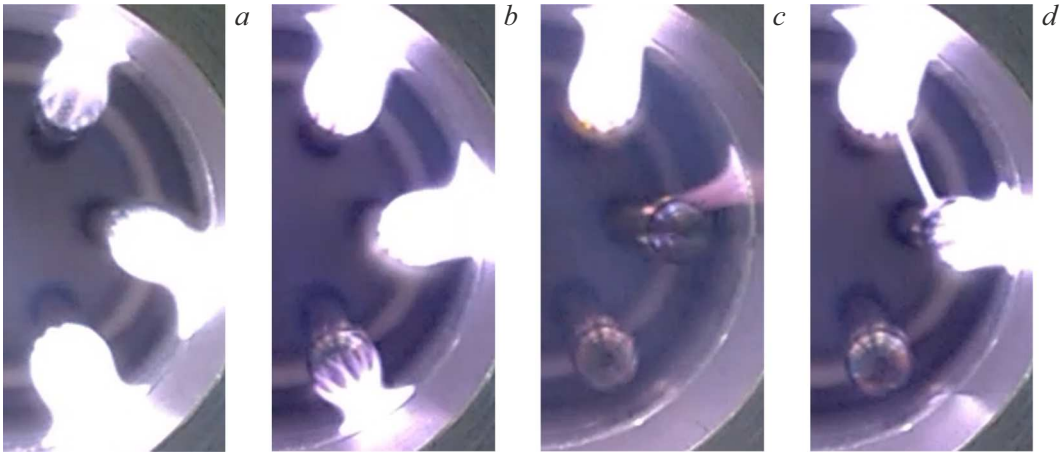

Figure 4. Microwave discharge in the multielectrode plasma torch (view from the outlet).

glow discharge in the form of a bright plasma filament is excited between the rounded end of the rod electrode and the inner wall of the discharge chamber (Fig. 4; see also [35]). This discharge covers the rounded electrode end almost completely and forms a round electrode spot approximately 4 mm in diameter on the inner wall of the discharge chamber. The discharge channel is compressed more than twofold in the central part of the interelectrode gap, forming a narrow bridge with uniform glow. Since the diameters of electrodes and the spot on the chamber wall are small compared to the internal diameter of the chamber, the curvature of the chamber wall in the spot region may be neglected, and it may be assumed that the discharge is initiated in the „hemisphere–plate" geometry of the interelectrode gap. The discharge channel was found to be split into filaments, which formed a self-similar (fractal) spatial structure, near the end of the rod electrode (Figs. 4, *a, b*). The ends of these filaments, which are in contact with the electrode surface, form a pattern of about 10^2 bright mobile microspots ordered into clusters with a triangular structure on this surface (Fig. 4, *a*). We believe that this distinct filamentation is attributable to the convex hemispherical shape of the electrode ends, which induces significant stretching of the discharge channel and makes individual filaments clearly visible. At the opposite end of the channel (near the chamber wall), the discharge filamentation was much less pronounced. However, chaotically moving bright microspots were also observed in the region of the electrode spot (Fig. 4, *c*). Note that such filamentation of the discharge channel is also typical of an atmospheric-pressure DC glow discharge (see, e.g., [39]). It follows from the results of spectral diagnostics and estimates obtained under similar experimental conditions that gas temperature T_g in the discharge channel is 1200 K, and the electron concentration and temperature are $n_e \sim 10^{15}-10^{16}\,\mathrm{cm}^{-3}$ and $T_e \sim 1\,\mathrm{eV}$, respectively [34,35]. In the pulse-periodic regime, single-channel sparks emerging at random between the electrodes were observed alongside the glow-type discharge channels (Fig. 4, *d*). These sparks appear due to the periodicity of magnetron operation and indicate that the formation of a glow-type channel is preceded by a spark breakdown at the leading edge of a pulse. The dynamics of discharge channels in both regimes was affected strongly by the gas-dynamic flow: its non-uniformity induced their displacement and oscillations. Comparing the examined microwave discharge regimes in the context of their practical application (e.g., for plasma treatment of materials), one may note that a higher concentration of active particles in a cold plasma jet may be obtained in the continuous current regime. Less pronounced heating of structural elements (electrodes, discharge chamber, etc.) of the torch and a lower temperature of the plasma jet are the advantages of the pulse-periodic regime, which may be critical for treatment of heat-sensitive materials.

Conclusion

Continuous and pulse-periodic regimes of excitation of an atmospheric-pressure microwave glow discharge in an electrode plasma torch in transverse argon flow were implemented by adjusting the magnetron power supply modes. The amplitude-time characteristics of the floating potential in a cold plasma jet of the microwave discharge were measured in these regimes. Fractal filamentation of the near-electrode regions of the discharge channel in the continuous regime was characterized. The obtained results suggest that a glow-type microwave discharge holds promise for production of wide cold plasma jets, which is of considerable interest in the context of development of plasma modification technologies for various materials.

Funding

This study was supported by a grant from the Russian Science Foundation (project No. 21-79-30062).

Conflict of interest

The authors declare that they have no conflict of interest.

References

[1] V.A. Trubnikov. *Fizicheskaya entsiklopediya* (Bol'shaya Ross. Entsikl., M., 1992), Vol. 3, p. 327 (in Russian).

[2] A.M. Kutepov, A.G. Zakharov, A.I. Maksimov. *Vakuumno-plazmennoe i plazmenno-rastvornoe modifitsirovanie polimernykh materialov* (Nauka, M., 2004) (in Russian).

[3] S. Vepřek, C. Eckmann, J.T. Elmer. Plasma Chem. Plasma Process., **8**, 445 (1988). DOI: 10.1007/BF01016059

[4] P. Favia, R. d'Agostino. Surf. Coat. Technol., **98** (1–3), 1102 (1998). DOI: 10.1016/S0257-8972(97)00285-5

[5] M. Dhayal, M.R. Alexander, J.W. Bradley. Appl. Surf. Sci., **252** (22), 7957 (2006). DOI: 10.1016/j.apsusc.2005.10.005

[6] Y. Deslandes, G. Pleizier, E. Poiré, S. Sapieha, M.R. Wertheimer, E. Sacher. Plasmas Polym., **3**, 61 (1998). DOI: 10.1023/B:PAPO.0000005939.84830.44

[7] N. Puač, Z.L. Petrović, M. Radetić, A. Djordjević. In *Materials Science Forum* (Trans. Tech. Publications Ltd, 2005), v. 494, p. 291. DOI: 10.4028/www.scientific.net/MSF.494.291

[8] A.I. Al-Shamma'a, S.R. Wylie, J. Lucas, J.D. Yan. IEEE Trans. Plasma Sci., **30** (5), 1863 (2002). DOI: 10.1109/TPS.2002.805371

[9] J. Hnilica, L. Potočňáková, M. Stupavsk., V. Kudrle. Appl. Surf. Sci., **288**, 251 (2014). DOI: 10.1016/j.apsusc.2013.10.016

[10] N. Srivastava, W. Chuji. Plasma Sci. Technol., **21** (11), 115401 (2019). DOI: 10.1088/2058-6272/ab3248

[11] J. Zhao, L. Nie. Phys. Plasmas, **26** (7), 073503 (2019). DOI: 10.1063/1.5092840

[12] M. Narimisa, F. Krčma, Y. Onyshchenko, Z. Kozáková, R. Morent, N. De Geyter. Polymers, **12** (2), 354 (2020). DOI: 10.3390/polym12020354

[13] S. Tiwari, A. Caiola, X. Bai, A. Lalsare, J. Hu. Plasma Chem. Plasma Process., **40**, 1 (2020). DOI: 10.1007/s11090-019-10040-7

[14] J. Batur, Z. Duan, M. Jiang, R. Li, Y. Xie, X.F. Yu, J.R. Li. Chem. Mater., **35** (10), 3867 (2023). DOI: 10.1021/acs.chemmater.2c03551

[15] X.P. Lu, Z.H. Jiang, Q. Xiong, Z.Y. Tang, X.W. Hu, Y. Pan. Appl. Phys. Lett., **92** (8), 081502 (2008). DOI: 10.1063/1.2883945

[16] R. Wang, H. Sun, W. Zhu, C. Zhang, S. Zhang, T. Shao. Phys. Plasmas, **24** (9), 093507 (2017). DOI: 10.1063/1.4998469

[17] M. Laroussi. Front. Phys., **8**, 74 (2020). DOI: 10.3389/fphy.2020.00074

[18] Y. Yu, K. Huang, L. Wu. Phys. Rev. E, **102** (3), 031201 (2020). DOI: 10.1103/PhysRevE.102.031201

[19] H.Y. Kim, S.K. Kang, S.M. Park, H.Y. Jung, B.H. Choi, J.Y. Sim, J.K. Lee. Plasma Process. Polym., **12** (12), 1423 (2015). DOI: 10.1002/ppap.201500017

[20] G. Xia, Z. Chen, A.I. Saifutdinov, S. Eliseev, Y. Hu, A.A. Kudryavtsev. IEEE Trans. Plasma Sci., **42** (10), 2768 (2014). DOI: 10.1109/TPS.2014.2329899

[21] M. Laroussi, T. Akan. Plasma Process. Polym., **4** (9), 777 (2007). DOI: 10.1002/ppap.200700066

[22] M. Laroussi, X. Lu. Appl. Phys. Lett., **87** (11), 113902 (2005). DOI: 10.1063/1.2045549

[23] K. Yambe, S. Satou. Phys. Plasmas, **23** (2), 023509 (2016). DOI: 10.1063/1.4942170

[24] Q.Y. Nie, Z. Cao, C.S. Ren, D.Z. Wang, M.G. Kong. New J. Phys., **11** (11), 115015 (2009). DOI: 10.1088/1367-2630/11/11/115015

[25] J.Y. Kim, J. Ballato, S.O. Kim. Plasma Process. Polym., **9** (3), 253 (2012). DOI: 10.1002/ppap.201100190

[26] M. Ghasemi, P. Olszewski, J.W. Bradley, J.L. Walsh. J. Phys. D: Appl. Phys., **46** (5), 052001 (2013). DOI: 10.1088/0022-3727/46/5/052001

[27] R. Wang, H. Xu, Y. Zhao, W. Zhu, C. Zhang, T. Shao. Plasma Chem. Plasma Process., **39**, 187 (2019). DOI: 10.1007/s11090-018-9929-8

[28] T. Shimizu, B. Steffes, R. Pompl, F. Jamitzky, W. Bunk, K. Ramrath, M. Georgi, W. Stolz, H.U. Schmidt, T. Urayama, S. Fujii, G.E. Morfill. Plasma Process. Polym., **5** (6), 577 (2008). DOI: 10.1002/ppap.200800021

[29] G. Isbary, J.L. Zimmermann, T. Shimizu, Y.F. Li, G.E. Morfill, H.M. Thomas, B. Steffes, J. Heinlin, S. Karrer, W. Stolz. Clin. Plasma Med., **1** (1), 19 (2013). DOI: 10.1016/j.cpme.2012.11.001

[30] T. Shimizu, Y. Ikehara. J. Phys. D: Appl. Phys., **50** (50), 503001 (2017). DOI: 10.1088/1361-6463/aa945e

[31] S. Arndt, A. Schmidt, S. Karrer, T. von Woedtke. Clin. Plasma Med., **9**, 24 (2018). DOI: 10.1016/j.cpme.2018.01.002

[32] T. Shimizu. Jpn. J. Appl. Phys., **59** (12), 120501 (2020). DOI: 10.35848/1347-4065/abc3a0

[33] V.M. Chepelev, A.V. Chistolinov, M.A. Khromov, S.N. Antipov, M.K. Gadzhiev. J. Phys.: Conf. Ser., **1556** (1), 012091 (2020). DOI: 10.1088/1742-6596/1556/1/012091

[34] S.N. Antipov, M.A. Sargsyan, M.K. Gadzhiev. J. Phys.: Conf. Ser., **1698** (1), 012029 (2020). DOI: 10.1088/1742-6596/1698/1/012029

[35] S.N. Antipov, M.Kh. Gadzhiev, M.A. Sargsyan, D.V. Tereshonok, A.S. Tyuftyaev, D.I. Yusupov, A.V. Chistolinov, A.G. Abramov, A.V. Ugryumov. Phys. Scr., **98** (2), 025604 (2023). DOI: 10.1088/1402-4896/acae65

[36] S.N. Antipov, V.M. Chepelev, M.K. Gadzhiev, A.G. Abramov, A.V. Ugryumov. Plasma Phys. Rep., **49** (5), 559 (2023). DOI: 10.1134/S1063780X23600299

[37] D.A. Mansfeld, A.V. Vodopyanov, S.V. Sintsov, N.V. Chekmarev, E.I. Preobrazhensky, M.E. Viktorov. Tech. Phys. Lett., **49** (1), 36 (2023). DOI: 10.21883/TPL.2023.01.55345.19384

[38] I.A. Ivanov, V.N. Tikhonov, A.V. Tikhonov. J. Phys.: Conf. Ser., **1393** (1), 012042 (2019). DOI: 10.1088/1742-6596/1393/1/012042

[39] A.V. Chistolinov, R.V. Yakushin, M.A. Sargsyan, M.A. Khromov, A.S. Tyuftyaev. J. Phys.: Conf. Ser., **1394** (1), 012006 (2019). DOI: 10.1088/1742-6596/1394/1/012006

Translated by D.Safin